Observations of the latitudinal structure of plasmaspheric convection plumes by IMAGE-RPI and EUV

Leonard N. Garcia,[1,2] Shing F. Fung,[2] James L. Green,[2] Scott A. Boardsen[2,3]
Bill R. Sandel,[4] and Bodo W. Reinisch[5]

Received 22 May 2002; revised 16 April 2003; accepted 2 May 2003; published 15 August 2003.

[1] Recent IMAGE Extreme Ultraviolet Imager (EUV) observations showed the first global images of plasmaspheric convection plumes, which have been interpreted as the plasmaspheric tails predicted theoretically 3 decades earlier. Using observations by the IMAGE Radio Plasma Imager (RPI), we show that these convection plumes have large latitudinal extent. These results complement those recently made by others in correlating IMAGE EUV data with measurements of total electron content in the ionosphere. By correlating in situ RPI density measurements with global plasmaspheric EUV images, we have shown that apparently detached plasma structures, as appear in RPI dynamic spectrograms, are in many cases plasmaspheric convection plumes. The temporal separation between the RPI and EUV observations help constrain the interpretation of one data set in the context of the other, thereby enabling an examination of the three-dimensional plasma density structures outside the core plasmasphere. The data sets are mutually reinforcing because the data are collected within a few hours of one another. We used the EUV data to provide unambiguous identification of density enhancements in the region outside the plasmasphere and used the RPI data to obtain accurate number densities and extend information from the EUV data set by measuring densities below the EUV sensitivity threshold. *INDEX TERMS:* 2768 Magnetospheric Physics: Plasmasphere; 2740 Magnetospheric Physics: Magnetospheric configuration and dynamics; 2730 Magnetospheric Physics: Magnetosphere—inner; 2788 Magnetospheric Physics: Storms and substorms; *KEYWORDS:* plasmasphere, plasmapause, inner magnetosphere, convection plumes, RPI, EUV

Citation: Garcia, L. N., S. F. Fung, J. L. Green, S. A. Boardsen, B. R. Sandel, and B. W. Reinisch, Observations of the latitudinal structure of plasmaspheric convection plumes by IMAGE-RPI and EUV, *J. Geophys. Res.*, *108*(A8), 1321, doi:10.1029/2002JA009496, 2003.

1. Introduction

[2] Density enhancements in the plasmatrough, i.e., the low-density region just outside of the plasmapause, have been identified by a variety of techniques for more than 30 years. These observations have been made from ion mass spectrometers on OGO-5 [*Chappell*, 1974; *Chen and Grebowsky*, 1974], and the Dynamics Explorer-1 spacecraft [*Horwitz et al.*, 1990], from electron densities inferred using UHR or plasma frequency measurements by ISEE-1 [*Carpenter et al.*, 1993], from sheath-induced potentials on the electric field experiment of Explorer 45 (S^3-A) [*Maynard and Chen*, 1975], and from ground-based studies of whistlers [*Ho and Carpenter*, 1976]. Over 3 decades of observations have provided a set of typical characteristics. The density enhancements are found predominantly in the dusk sector, often after moderate to disturbed magnetic activity conditions. They have a variety of sizes and densities and can corotate during quiet conditions [*Taylor et al.*, 1971].

[3] Convection models have been used to understand the global characteristics of these time-dependent plasma features. The large-scale shape of the plasmasphere is largely defined by the interaction of the solar wind influenced dawn-dusk electric field and the corotational electric field. Models that introduce temporal or spatial variations in the dawn-dusk electric field and subsequent changes in the strength of the sunward convective flow of plasma can replicate some of the features of the observed density enhancements. These models indicate that the density enhancements are signatures of a Sun-pointing plasma convection tail extending from and joined to the duskside plasmasphere [*Grebowsky*, 1970; *Chen and Grebowsky*, 1974; *Grebowsky and Chen*, 1976]. The models indicate that variations in the convection field can lead to complex plasma structures with multiple plumes forming and wrapping around the main body of the plasmasphere during quiet periods [*Chen and Wolf*, 1972; *Horwitz et al.*, 1990]. These plasma convection tails are referred to in this paper as

[1]QSS Group, Inc., Lanham, Maryland, USA.
[2]NASA Goddard Space Flight Center, Greenbelt, Maryland, USA.
[3]L-3 Communications EER Systems, Inc., Largo, Maryland, USA.
[4]Lunar and Planetary Laboratory, The University of Arizona, Tucson, Arizona, USA.
[5]Center for Atmospheric Research, University of Massachusetts, Lowell, Massachusetts, USA.

0148-0227/03/2002JA009496$09.00

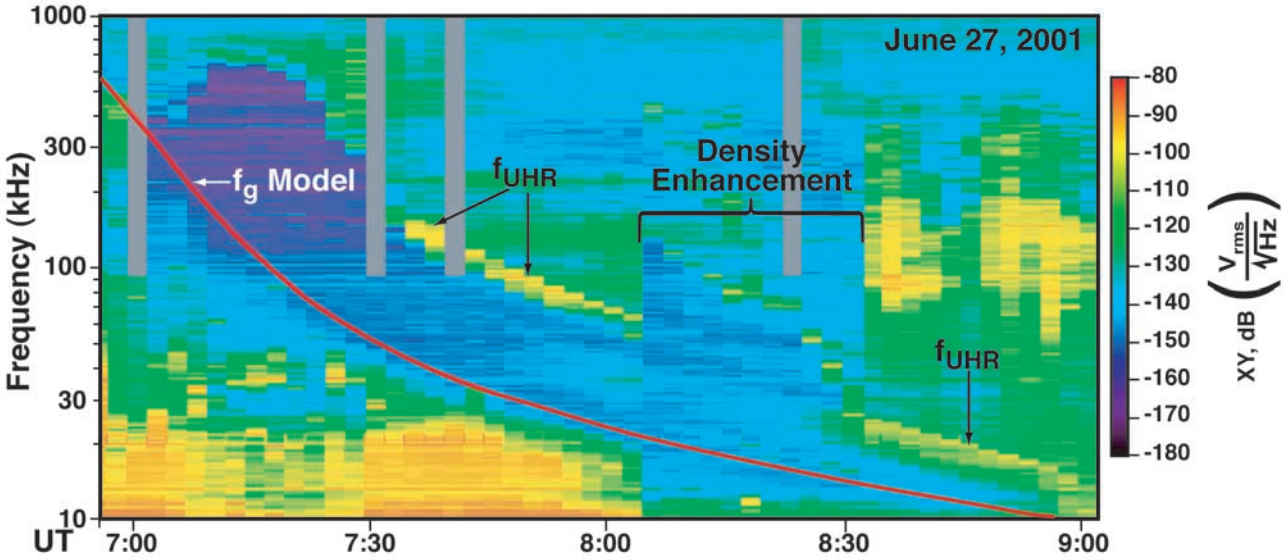

Figure 1. The dynamic spectrogram of IMAGE-RPI passive noise data over about 2 hours on 27 June 2001. Frequency is in units of kilohertz; time is in UT. Frequency resolution between 20 kHz and 1 MHz is 2% and time resolution is between 2 and 5 min. The colors indicate the combined amplitude of the X and Y antennas. Over the time period shown in this figure the MLT of the spacecraft was ~18. IMAGE was on an outbound pass crossing through the plasmasphere between roughly 0700 and 0730 UT. Between 0800 and 0830 UT IMAGE passed through a plasma density enhancement in the trough which we interpret as a plasma convection plume. Overlaying the figure is a curve indicating the modeled gyrofrequency (f_g) through this region. The bright line in the plasmatrough we interpret as the upper hybrid resonance frequency (f_{UHR}) which was used with the modeled gyrofrequency to compute the electron density profile.

plasma convection plumes to distinguish more clearly these structures from the geomagnetic tail.

[4] The Imager for Magnetopause-to-Auroral Global Explorer (IMAGE) spacecraft was launched into a polar orbit on 25 March 2000. The apogee of 8.2 R_E geocentric radial distance was initially set towards the dayside near-noon meridian, with a perigee of 7400 km and a 14.25 hour orbital period. The Radio Plasma Imager (RPI) instrument on IMAGE consists of two 500 m antennas (along the X and Y axis) in the spin plane of the spacecraft and a 20 m antenna (along the Z axis) aligned with the satellite spin axis [*Reinisch et al.*, 2000]. On 3 October 2000 the X antenna snapped to a length of 325 m with minimal impact to instrument performance. RPI is a low power radio sounder operating in the frequency range of 3 kHz to 3 MHz and is capable of sending radio frequency pulses to actively probe various regions of the magnetosphere. RPI can also operate as a passive noise receiver making in situ measurements of the local plasma. In its passive mode, the RPI instrument produces dynamic spectrograms that are the primary source of data for this study. These spectrograms have a time resolution of between 2 and 5 min and a frequency resolution of 400 Hz between 3 and 20 kHz and 2% between 20 kHz and 1 MHz.

[5] The RPI dynamic spectrograms have recorded many solar Type III radio bursts, auroral kilometric radiation and nonthermal continuum emissions [*Reinisch et al.*, 2001; *Fung et al.*, 2002; *Galkin et al.*, 2001]. These spectrograms also show that IMAGE has often passed into enhanced plasma regions that are well above the average densities in the trough and much higher than expected using current power law descriptions for trough densities [*Carpenter and Anderson*, 1992; *Sheeley et al.*, 2001]. Often visible in these spectrograms as well is a bright narrow-band plasma line, which effectively yields total electron density. This line has been interpreted as being near the upper hybrid resonance (UHR) [*Mosier et al.*, 1973; *Gurnett et al.*, 1979].

[6] The IMAGE spacecraft carries several other instruments including the Extreme Ultraviolet Imager (EUV) [*Sandel et al.*, 2000]. This instrument consists of a set of three cameras tuned to detect solar radiation resonantly scattered at 30.4 nm by He^+. Data from the three cameras are combined to form a single global image of the ionized helium distribution in the plasmasphere. EUV observations are made over several hours around apogee. These images are generally taken at high northern latitudes and have a time resolution of 10 min and a spatial resolution of 0.1 R_E. Time-lapsed images show the motion of enhanced and depleted regions in the plasmasphere and plasma convection plumes, as well as other recurrent structures [*Sandel et al.*, 2001]. The purpose of this paper is to examine the local and global characteristics of plasma convection plumes, to investigate the advantages gained by combining the RPI and EUV archives for the study of plasma convection plumes observed in common, and to illustrate how RPI and EUV data supplement one another adding a global perspective to the RPI data and extending the sensitivity limit to EUV data.

2. Study Background

[7] This study began with a search through the IMAGE RPI and EUV archives from January–December 2001 for dense plasma features outside of the plasmasphere in the

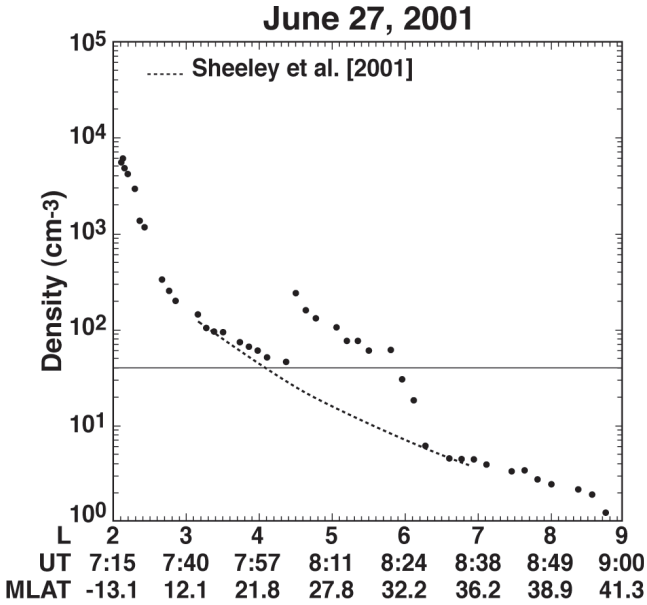

Figure 2. The electron density profile derived from the dynamic spectrogram shown in Figure 1. The estimated uncertainty in the electron number density is less than 10%. The horizontal line at 40 cm^{-3} indicates the EUV sensitivity threshold estimated by *Goldstein et al.* [2003]. Also shown is a model of trough densities derived from CRRES data by *Sheeley et al.* [2001].

plasmatrough. The EUV data used for this study are movies composed of successive EUV images each one of which is a 10 min integration. There are 558 such movies for the year 2001 composed of 21,500 frames for a total observing time of over 3000 hours. Our survey of the data resulted in the identification of 43 plumes. For the same period of time there are 88 structures in the RPI dynamic spectrograms that indicate enhanced density structures in the trough or large irregularities in the plasmapause. For these combined data sets there are ten events in which it can be shown that both RPI and EUV observed the same plasma convection plume. For this analysis two techniques have been used. First, if the IMAGE ephemeris data show that the spacecraft passed through the same range of longitudes as the EUV-observed structure at the same time that RPI observed a density enhancement then we infer that the feature observed by RPI and EUV is the same. Second, using the RPI-derived electron number densities, we model what EUV would expect to see if the He^+ were distributed in the same way and assuming that the densities are constant along a field line. The model is then compared with He^+ column densities derived from the EUV images at lines of sight corresponding to the positions of the RPI measurements along the IMAGE trajectory.

2.1. Longitude Comparison of RPI and EUV-Observed Features

[8] To determine whether IMAGE passed through the plasma plume, our analysis software computes the magnetic longitude, in Geomagnetic (MAG) coordinates, and the L-shell for each user-selected pixel in the EUV images and maps them onto the magnetic equatorial plane. The choice of where to select points in the EUV global plasmasphere images is fairly reproducible but not precise. A boundary edge is chosen based on its color, the color indicating an equal light intensity contour or isophote. A potential source of error in this approach is that, given the long path length of He^+ through the plasmasphere, the peaks in the contribution function for lines of sight along a given isophote may lie at different distances from the spacecraft and hence correspond to different plasma structures. Our analysis software determines the minimum L-shell value along the line-of-sight for each pixel selected using a tilted dipole magnetic field model. By mapping such tangent points onto the equatorial plane, the location of features in the image can be estimated. This mapping technique is similar to that performed by others [*Spasojevic et al.*, 2002]. *Goldstein et al.* [2003] have shown that, by selecting the boundary in EUV images that shows the steepest brightness gradients, the plasmapause can be reliably identified. They estimated the uncertainty in selecting the plasmapause in this way to be about 0.2 R_E for a well-defined plasmapause. Using our sampling technique as described above, samples were taken along a single

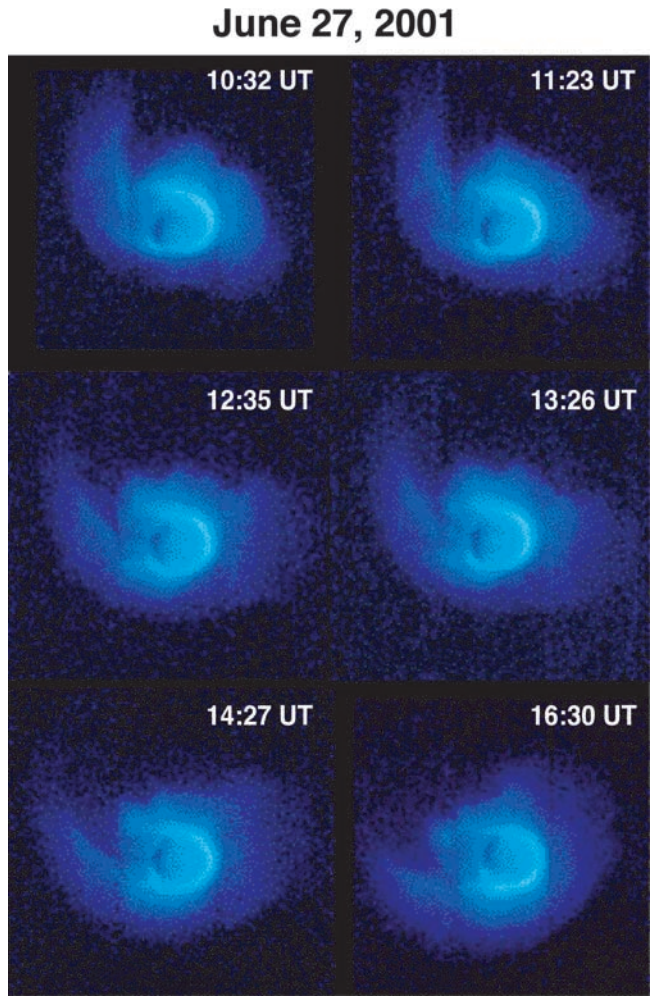

Figure 3. A sequence of six EUV global images of the plasmasphere each roughly 1 hour apart from 1032 to 1630 UT on 27 June 2001. The Sun is toward the right. This sequence illustrates the motion of the plasma plume from the evening towards the morning sector. The first image was taken about 2 hours after IMAGE passed through the RPI-observed density enhancement shown in Figure 1.

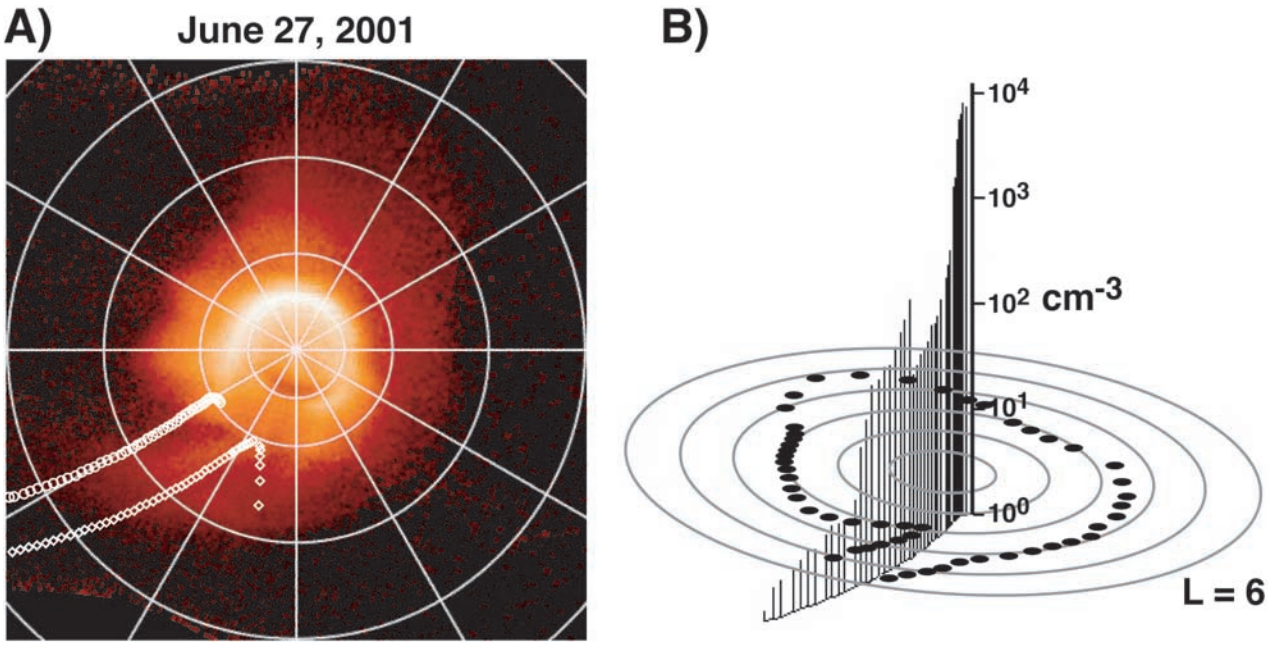

Figure 4. (a) EUV image for 27 June 2001 mapped to the plane of the magnetic equator. The large circles mark L = 1, 2, 4, 6, and 8. The azimuthal coordinate is magnetic longitude, with zero at the right. RPI recorded the electron density at the [L, longitude] positions marked by white diamond symbols (but far from the plane of the magnetic equator). The white circles mark the path from which the He^+ column abundances in the bottom panel of Figure 5 were taken. The Sun is near magnetic longitude 80 degrees. (b) Samples from Figure 4a (filled circles) of the plasmapause and plasma plume are mapped into [L, magnetic longitude] coordinates. The concentric rings are at L = 1 through 6. The vertical bars plotted along the orbital path of IMAGE are the electron number densities from Figure 2. The location of the density enhancement observed by RPI between 0800 and 0830 UT is shown to coincide with the plasma plume observed by EUV.

isophote outlining much of the plasmasphere and plasma plume. The longitude of the IMAGE spacecraft during the RPI-observed density enhancement is then compared to the longitude of the features selected from the EUV images. This comparison is made assuming that the plume is in corotation between the time IMAGE passes through the enhancement and EUV begins observing the plasmasphere.

2.2. Modeling EUV Observations Based on RPI Density Measurements

[9] Electron density in the plasma plume structures can be inferred along the orbital path of IMAGE using the RPI passive noise dynamic spectrograms. The strong plasma line often observed in the plasmasphere and detached density structures is interpreted to be the upper hybrid resonance (UHR). In those regions where the line is less prominent we used steep intensity gradients in the spectrograms as an aid to identifying the UHR. From the UHR frequency and the gyrofrequency the plasma frequency and subsequently the electron number density are determined. Modeled values of the local electron gyrofrequency (f_g) are used in the calculation of electron number density. These values of f_g are based on the T96_01 magnetic field model [*Tsyganenko*, 1995]. The upper hybrid resonance frequency (f_{UHR}) is related to the electron gyrofrequency (f_g) and plasmafrequency (f_p) by

$$f_p^2 = f_{UHR}^2 - f_g^2$$

The electron number density (n_e) in cm^{-3} is then determined by

$$n_e = \left(\frac{\pi\, m_e f_p^2}{e^2}\right) \approx \left(\frac{f_p}{8980}\right)^2,$$

where m_e is the mass of the electron, e is the charge of the electron, and f_p is the electron plasmafrequency in Hz.

[10] RPI electron density profiles of the plasmasphere have been compiled for most of the spectrograms obtained to date. We estimate the uncertainty in these number densities to be less than 10% during quiet periods. These data compare well with existing models of plasma density distributions and show large-scale variations as functions of solar wind and geomagnetic activity [*Fung et al.*, 2001].

[11] To compare the structures measured by EUV and RPI, we must account for differences in the quantities measured by the two instruments. RPI measures the in situ electron density, while EUV measures the column abundance of He^+ along the lines of sight corresponding to each pixel. For our comparison we use a simple model of the distribution of He^+ to estimate what EUV would see under the assumptions that (1) the distribution of He^+ in the equatorial plane is proportional to the electron density measured by RPI, and (2) the He^+ density along a flux tube is constant. The model performs line-of-sight integrations of the specified electron density, and hence predicts electron column abundance, and under assumption 1 above the He^+

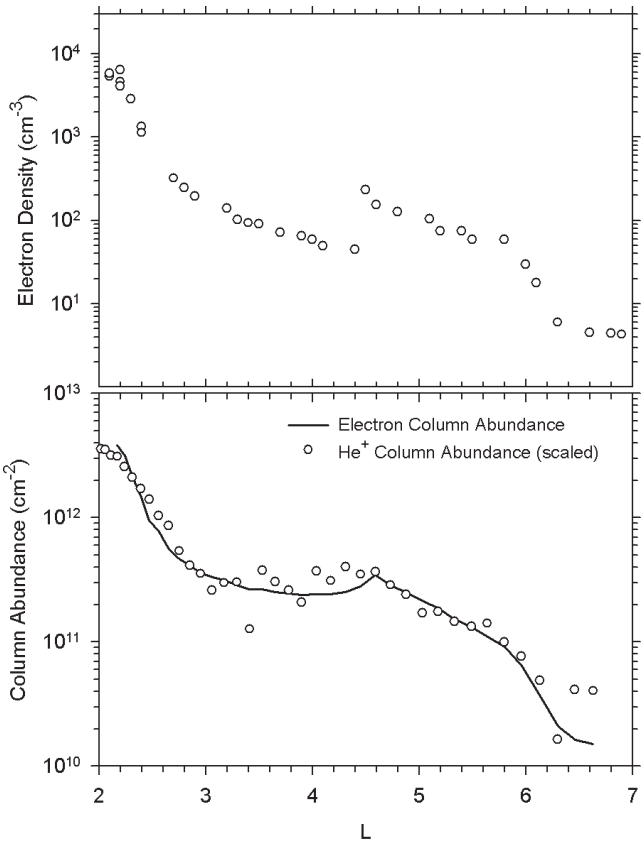

Figure 5. (top) Electron density measured by RPI at the positions shown by white diamonds in Figure 4a. (bottom) Electron column abundance computed from the electron density profile in the top panel, compared with the He^+ column abundance. The values for the He^+ column abundance come from the positions marked by open circles in Figure 4a. Their ordinates have been scaled to match the electron column abundance profile.

30.4-nm intensities for comparison with the measured EUV image. The model line-of-sight integration excludes the region of Earth's shadow because He^+ in the shadow does not emit 30.4-nm light.

[12] We expect imperfect agreement between measured and modeled brightness profiles, owing to the dynamic character of the plasmasphere. For the four cases that we consider in detail here, the EUV and RPI measurements were separated by 3 to 5 hours. Our experience with imaging the plasmasphere suggests that in these intervals, changes in structure and density arising from radial motions or differential rotation are likely. This is particularly true of the dusk through midnight sectors, where plumes most often appear and where our measurements were made. EUV images show that the plasma in this region is often neither corotating nor fixed in local time but rather moving with an intermediate angular velocity. Refilling from the ionosphere can also contribute to time variations. Finally, the modeled and observed profiles may differ because our assumption of constant density along the flux tube is an over-simplification. In comparing the fit of brightness profiles measured by EUV and inferred from RPI measurements, we recognize that structures in the plasmasphere may maintain their general shape as they drift in MLT and magnetic longitude. Therefore small deviations between the regions sampled by EUV and RPI may be needed to achieve a good match.

3. IMAGE Passes Through the Plasma Convection Plume

3.1. 27 June 2001

[13] IMAGE-RPI observed a sharp density enhancement within the plasmatrough from 0804 through 0827 UT during an outbound pass. The spacecraft at this time was in the dusk sector at ~1800 MLT and passed through L shells from 4.5 to 6.1. On the previous day Kp had peaked at 4.0 and dropped to a value of 1.3 by the time of this event. As seen in the spectrogram in Figure 1, IMAGE crossed the plasmapause boundary around 0730 UT. The electron number density dropped sharply at this boundary and continued to drop more gradually as the spacecraft moved through the plasmatrough region and on towards apogee. Shortly after 0800 UT, the spacecraft encountered a sharp increase in electron number density after which the densities again slowly decreased. The morphology of this enhancement is similar to those seen in ISEE-1 data at similar L ranges and MLT [*Carpenter et al.*, 1993]. *Carpenter et al.* [2000] also report similar structures in CRESS data and discuss the physical processes that may lead to the formation of these steep walls including shear flows from sub auroral ion drifts. Figure 2 is the electron number density profile derived by selecting from Figure 1 the strong plasma line that we estimate to be near the upper hybrid resonance frequency and using the technique described in section 2.2. The plasmapause is indicated in Figure 2 by the sharp drop in density between L = 2.2 and 2.7. The density enhancement in the trough is visible at L about 4.5. Comparison of the observed number densities with the plasmatrough model of *Sheeley et al.* [2001] shows both that our density estimates through most of the plasmatrough are consistent with the model and that the density enhancement was well above the model and remained high until about 0830 UT at which point the spacecraft was at L = 6.3. The horizontal line represents an estimate of the EUV sensitivity threshold (40 ± 10 cm^{-3}) by *Goldstein et al.* [2003].

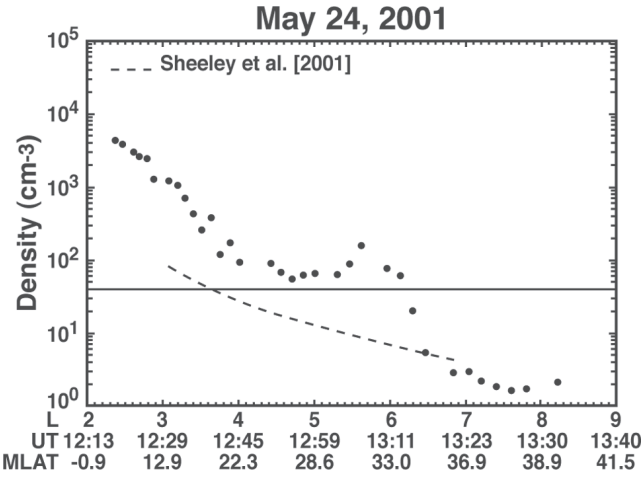

Figure 6. An electron density profile similar to Figure 2 for 24 May 2001. RPI detected a density enhancement in the plasmatrough between L = 5.5 and 6.5.

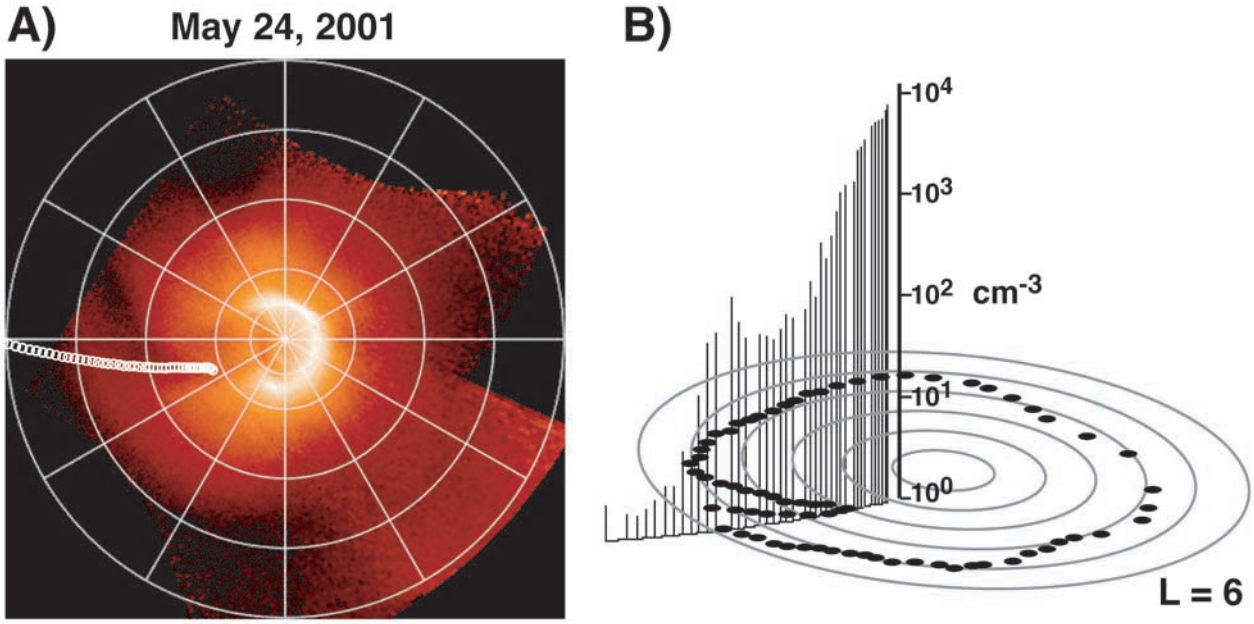

Figure 7. (a) EUV image for 24 May 2001 mapped to the plane of the magnetic equator. The large circles mark L = 1, 2, 4, 6, and 8. The azimuthal coordinate is magnetic longitude, with zero at the right. RPI recorded the electron density at the [L, magnetic longitude] positions marked by white circles (but far from the plane of the magnetic equator). The Sun is near magnetic longitude 16 degrees. (b) Samples from Figure 7a (filled circles) of the plasmapause and plasma plume are mapped into [L, magnetic longitude] coordinates. The concentric rings are at L = 1 through 6. The vertical bars along the orbital path of IMAGE are the electron number densities from Figure 6. The location of the density enhancement observed by RPI is shown to coincide with the plasma plume observed by EUV.

[14] EUV began observing the plasmasphere about one hour after IMAGE passed through the density enhancement. Figure 3 is a sequence of 6 EUV global images of the plasmasphere each roughly 1 hour apart from 1032 to 1630 UT on 27 June 2001. The Sun is toward the right. This sequence shows a plasma plume extending out from the core plasmasphere and over 6 hours moving from the evening towards the morning sector.

[15] The EUV image in Figure 4a is a summation of four single frames taken from 1131 to 1202, approximately 4 hours after the RPI measurements. Before summing, the individual images were mapped to the plane of the magnetic equator in [L, magnetic longitude] space using the technique described by *Sandel et al.* [2003]. Figure 4b is a polar plot of the samples (filled circles) outlining the plasmasphere and plume in Figure 4a. The vertical bars are the electron density profile from Figure 2 displayed along the projection of the orbital path of IMAGE. The radial coordinate is L-shell and the azimuthal coordinate is magnetic longitude. The plume is assumed to have maintained corotation between the time of the IMAGE passage through the structure and the time of this EUV observation. The plume is roughly 1.5 R_E in radial extent at its widest point. The fact that the longitude of the spacecraft where RPI detected the density enhancement matches that of the plasma plume seen in the EUV image is evidence that the RPI-observed enhancement was a plasma plume. The peak density of the plume along the spacecraft trajectory was 200 cm^{-3}.

[16] The electron density profile in the top panel of Figure 5 is the same as that in Figure 2. It shows a step near L = 4.4 that is reflected in a weak peak in the electron column abundance near the same radial position (the solid line in the bottom panel of Figure 5). As described in section 2.2, the solid line in the bottom panel of Figure 5 shows what EUV would observe had the He^+ been distributed the same way as the electrons. The EUV image shows that the He^+ distribution at the same longitudes and about 4 hours later was relatively unstructured. However, the brightness profile taken along the path marked by the + symbols in Figure 4a, shown by open circles in the bottom of Figure 5, has structure similar to that of the electron column abundance. That path is a translation without rotation of the RPI path, toward lower values of magnetic longitude. Plasmaspheric features that are fixed in magnetic local time move toward lower magnetic longitude with increasing time, so this shift is consistent with the common tendency toward subcorotation for plumes in this range of local times. This shift suggests that the feature moved at a rate that was intermediate between corotating and fixed in local time, roughly 2/3 of the corotation velocity. Some change of shape of the plume owing to differential subcorotation is expected and apparently occurred because a simple rotation of the path in magnetic longitude is not sufficient to achieve a good match of electron and He^+ column abundances.

3.2. 24 May 2001

[17] Taken from 1300 to 1312 UT on an outbound pass, approximately 15 min after having crossed the plasmapause, the RPI electron density profile seen in Figure 6 shows that IMAGE passed through an enhanced density region. The peak density is estimated to have been nearly 200 cm^{-3}. The IMAGE spacecraft was at ~2000 MLT passing through L values between 5.2 and 6.1. Kp had peaked at about 3.3 the

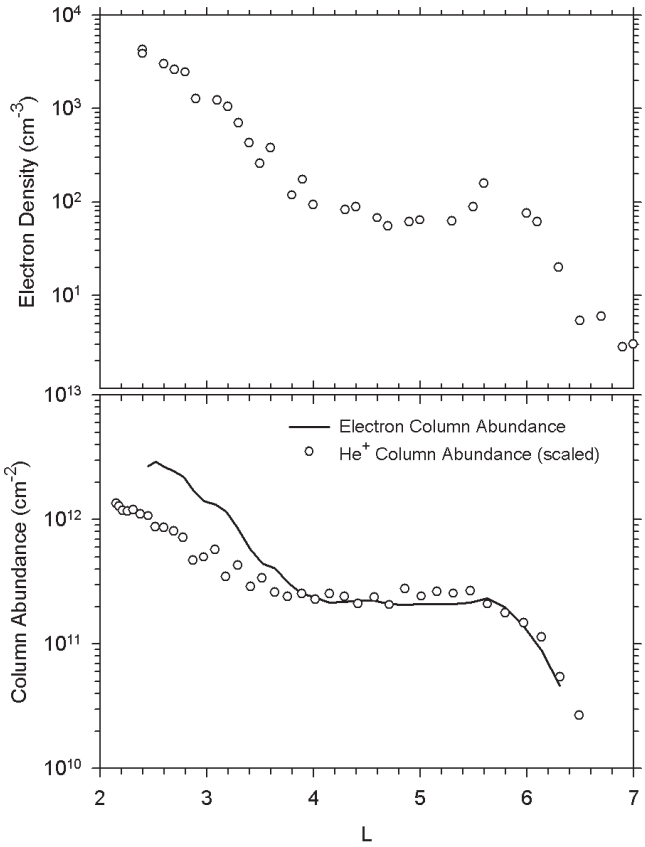

Figure 8. (top) Electron density measured by RPI at the positions shown in Figure 7a. (bottom) Electron column abundance computed from the electron density profile in the top panel, compared with the He^+ column abundance. The values for the He^+ column abundance come from the positions marked in Figure 7a. Their ordinates have been scaled to match the electron column abundance profile.

day before and had been in decline throughout the past 24 hours. Kp was about 1.0 at the time of this event. EUV began observations about one hour after passing through this feature. The EUV image in Figure 7a is a sum of four single frames from the period 1527–1558 UT, approximately 4 hours after the corresponding RPI measurements. The image shows a plasma plume that probably formed near the dusk sector several hours earlier and has rotated to the midnight sector. There is a region here that is distinctly reduced in helium density that separates the plume from the rest of plasmasphere and forms a notch at the base of the plasma plume. Over 5 hours of EUV images show this dark notch moving through the dawn sector. It is highly likely that IMAGE passed through this plasma plume based on a comparison of magnetic longitudes of the plume with the orbital position of IMAGE during the RPI-observed density enhancement (see Figure 7b).

[18] The top panel of Figure 8 shows the electron density measured by RPI at the positions marked by plus symbols in Figure 7a. Owing to the line-of-sight integration, the column abundance computed by our model from this electron density profile (bottom panel) is smoother than the electron density profile, with structure of much lower amplitude. We derived the He^+ column density by sampling the image in Figure 7a at the same values of L and magnetic longitude for which RPI measured the electron density. The similarity of the shapes between L = 4 and L = 6.5, where the structure in the electron density profile appears, is quantitative evidence that the two instruments observed the same features of the plasmasphere.

3.3. 1 October 2001

[19] From 0940 to 1005 UT, IMAGE-RPI detected another density enhancement in the plasmatrough during an outbound pass. The spacecraft was in the early afternoon sector at ~1300 MLT crossing L-shells between 4.3 and 5.9. This was during a time period of elevated Kp values (Kp = 5.7). The Kp average for the previous 24 hours was 4.7. The shape of the enhanced region, seen in the electron density profile in Figure 9, was more irregular than for the case on 27 June 2001. The peak density appeared to be lower as well, approximately 60 cm^{-3}. EUV began observing about an hour after exiting this enhanced region. To avoid damage from sunlight during this time, the gain of the cameras was reduced for part of each spin. Despite this fact, a sunward pointing plasma convection plume is discernable on the dusk side of the plasmasphere as shown in Figure 10a. Figure 10a is a summation of four single frames taken from 1201 to 1232 UT, approximately 3 hours after the RPI observations. Only the base of the plume is clearly visible because of the viewing angle of IMAGE at the time and due to protection against sunlight. Using the same mapping technique mentioned above, the longitude of the base of this plume was compared to the IMAGE orbital path during the time of the RPI-observed density enhancement (see Figure 10b). Unfortunately, much of the path sampled by RPI is near the upper edge of the useful part of the EUV image. At this time, that part of the image is not photometrically reliable because switching the detector high voltage to avoid scattered sunlight reduced the effective exposure time there. For this reason, column abundances and brightness profiles along the RPI path could not be obtained.

4. Discussion

[20] The unique perspective of the EUV cameras combined with the high sensitivity of the RPI receivers provides

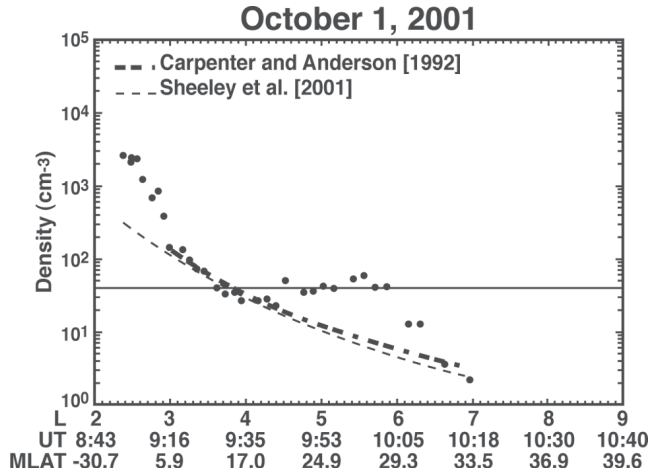

Figure 9. An electron density profile similar to Figure 2 for 1 October 2001. RPI detected a density enhancement in the plasmatrough between L = 4.5 and 6.2. Also shown are models of plasmatrough densities from *Carpenter and Anderson* [1992] and *Sheeley et al.* [2001].

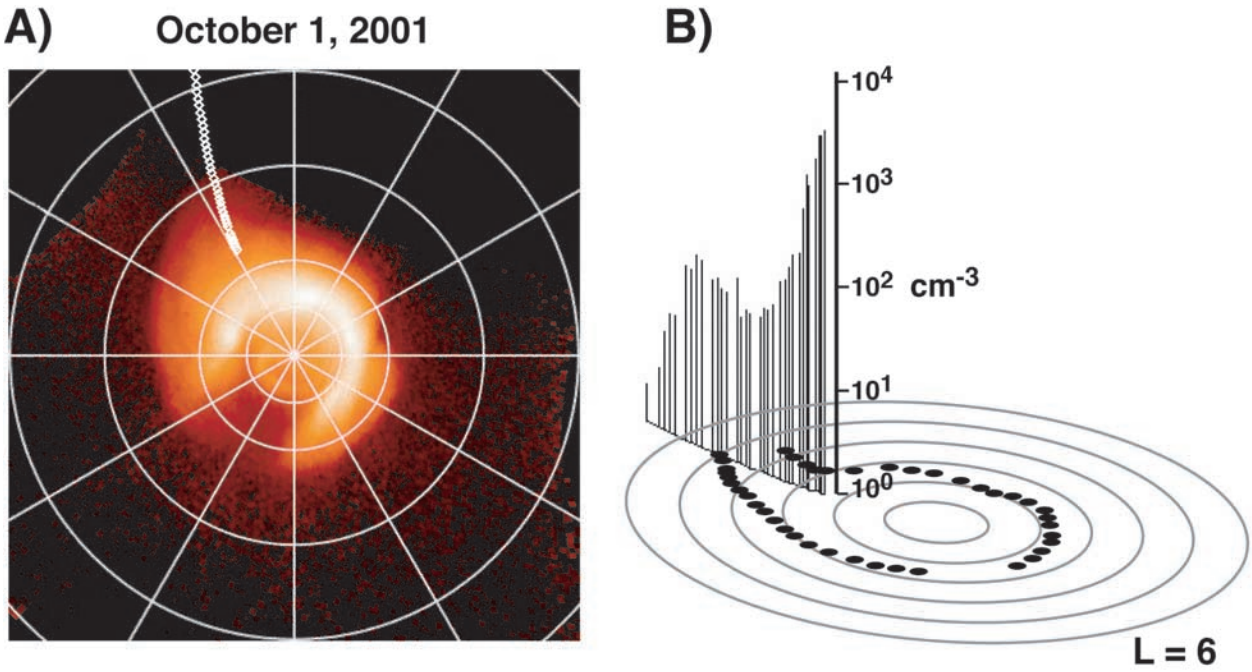

Figure 10. (a) EUV image for 1 October 2001 mapped to the plane of the magnetic equator. The large circles mark L = 1, 2, 4, 6, and 8. The azimuthal coordinate is magnetic longitude, with zero at the right. RPI recorded the electron density at the [L, longitude] positions marked by "x" symbols (but far from the plane of the magnetic equator). The Sun is near magnetic longitude 65 degrees. (b) Samples from Figure 10a (filled circles) of the plasmapause and plasma plume are mapped into [L, magnetic longitude] coordinates. The concentric rings are at L = 1 through 6. The vertical bars along the orbital path of IMAGE are the electron number densities from Figure 9. The location of the density enhancement observed by RPI is shown to coincide with the plasma plume observed by EUV.

the ability to investigate both the global dynamics of the plasmasphere and localized density structures. The EUV imager has observed many examples of plasmasphere convection plumes [*Sandel et al.*, 2001], which had been discussed for some time in the literature [e.g., *Grebowsky*, 1970] but never before had global images of these structures been seen. Combining these data with the passive noise observations of RPI enables direct determination of the electron number density and structural characteristics of the plume along the orbit path of IMAGE. Table 1 is a summary of the three plasma convection plume crossings discussed in the text as well as seven other plume crossings in 2001 for which there is a strong correlation between RPI and EUV. These plume crossings cover a range of magnetic local times, mostly in the afternoon to evening sectors. The crossings occur mostly at magnetic latitudes between 20 and 35 degrees although there is one case of a plume crossing near the equatorial plane.

[21] Several of our selected IMAGE spacecraft crossings are in the plasmatrough region. A few plume crossings, however, coincide with what appeared in the spectrograms as deep density variations inside the plasmasphere. Many of these depleted density regions have been interpreted as being cavities within the plasmasphere or as narrow troughs separating the main plasmasphere from a plasma plume connected to the main plasmasphere [*Carpenter et al.*, 2000]. These two interpretations may describe different stages in the same erosion process of the plasmasphere.

Table 1. Characteristics of Selected Plasma Convection Plumes Observed By IMAGE RPI/EUV During 2001

Date in 2001	Time (UT)		L range	MLT	Geomagnetic Latitude Range	Max. n_e Along Path, cm^{-3}	Kp During IMAGE Pass	Peak (Avg.) Kp Previous 24 Hours
	RPI	EUV						
13/14 March		1057–1249	3.0–3.6	1.4	18.0–23.0	1300	1.3	3.7 (2.6)
	1821–1830	2321–0013						
13 April	1405–1420	1702–2036	2.1–2.7	23.5	−4.5–11.0	2700	5.7	7.3 (2.7)
9 May	1632–1636	0600–1341	2.7–3.0	21.9	8.0–11.5	2300	5.3	5.0 (4.3)
24 May	1300–1312	1529–1904	5.2–6.1	20	29.0–33.0	200	1.0	3.3 (2.0)
10 June	1730–1734	1921–0322	4.6–5.0	20.2	28.5–30.5	100	2.7	5.7 (4.0)
27 June	0804–0827	1022–1823	4.5–6.1	18	25.0–33.0	200	1.3	4.0 (1.3)
16 July	0748–0806	1020–1415	5.5–7.0	17	29.0–34.0	96	1.7	3.7 (2.7)
23 August	0728–0738	1111–1334	8.4–9.2	14.8	37.0–38.0	11	2.7	4.3 (3.7)
24/25 September		1047–1351	5.5–6.0	12.5	32.0–34.5	90	0.7	4.3 (2.4)
	2112–2119	0135–0230						
1 October	0940–1005	1153–1630	4.3–5.9	13	19.0–29.0	60	5.7	6.0 (4.7)

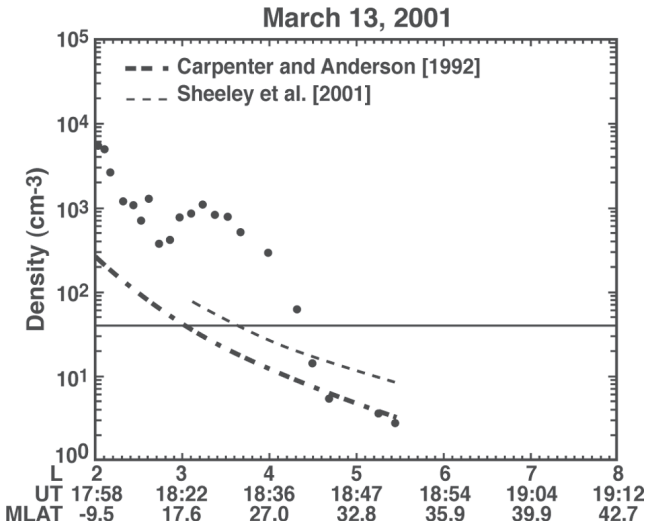

Figure 11. An electron density profile similar to Figure 2 for 13 March 2001. RPI detected a density enhancement between L = 3 and 4. Also shown are models of plasmatrough densities from *Carpenter and Anderson* [1992] and *Sheeley et al.* [2001].

Discrimination between the two models is possible using the techniques described above. On 13 March 2001, for example, the RPI data reveals a deep density depletion beginning around 1810 UT at a magnetic local time of 0124 (see Figure 11). The outlying structure has a peak density ~3 times the density within the depletion region. A comparison of the IMAGE trajectory with the EUV data indicates that the IMAGE orbit apparently crossed close to the leading edge where a plasma plume attaches to the plasmasphere (see Figure 12). At 1840 IMAGE crosses the outer edge of this plume. EUV recorded a well-developed plasma plume extending from the premidnight sector through dusk. A dark channel separated the plume from the main plasmasphere. The image in Figure 12a is a summation of 4 single frames taken from 1218 to 1250 UT, approximately 5 hours prior to the corresponding RPI measurements of electron density. The structure in the electron density profile leads to a more pronounced dip in the electron column abundance (bottom panel of Figure 13), which matches the shape of the measured He^+ column abundance well. The He^+ profile has been shifted to lower L by 1 unit. Because the EUV observation preceded the RPI measurement, this adjustment corresponds to inward motion of the measured features, the bright plume and dark channel. This is not unusual behavior for structures in this local time sector.

[22] A comparison of Kp values during the times of the plume crossings shows that most occurred in a declining phase several hours after a peak in Kp. Peaks in Kp indicate a strengthening of the convection electric field. This causes the formation of the plasma convection plume on the dusk side and the draining of plasma away from the plasmasphere in the sunward direction. Decline in Kp indicates a weakening of the convection electric field. A plume formed

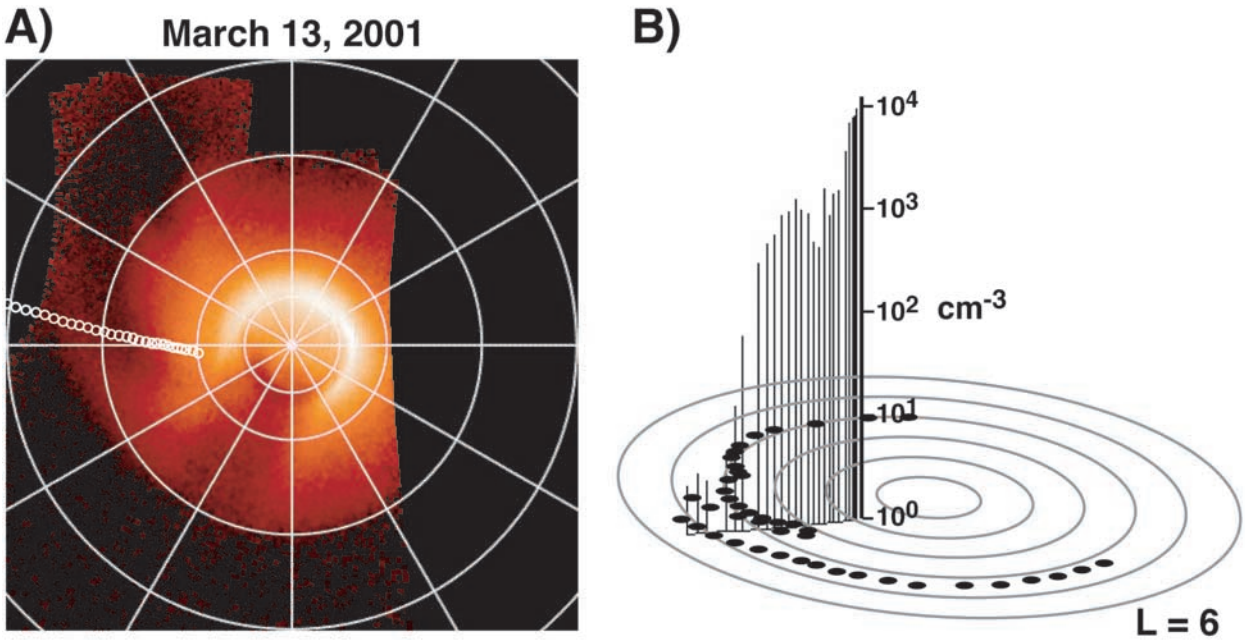

Figure 12. (a) EUV image for 13 March 2001. The range of L is to 6 rather than 8 as in Figure 7a. The Sun is near magnetic longitude 65 degrees, and a plasma plume extends from premidnight through the dusk sector. The white circles mark positions of RPI electron density and EUV He^+ column abundance measurements. (b) Samples from Figure 12a (filled circles) of the plasmapause and plasma plume are mapped into [L, magnetic longitude] coordinates. The concentric rings are at L = 1 through 6. The vertical bars along the orbital path of IMAGE are the electron number densities from Figure 11. The location of the density enhancement observed by RPI is shown to coincide with the plasma plume observed by EUV.

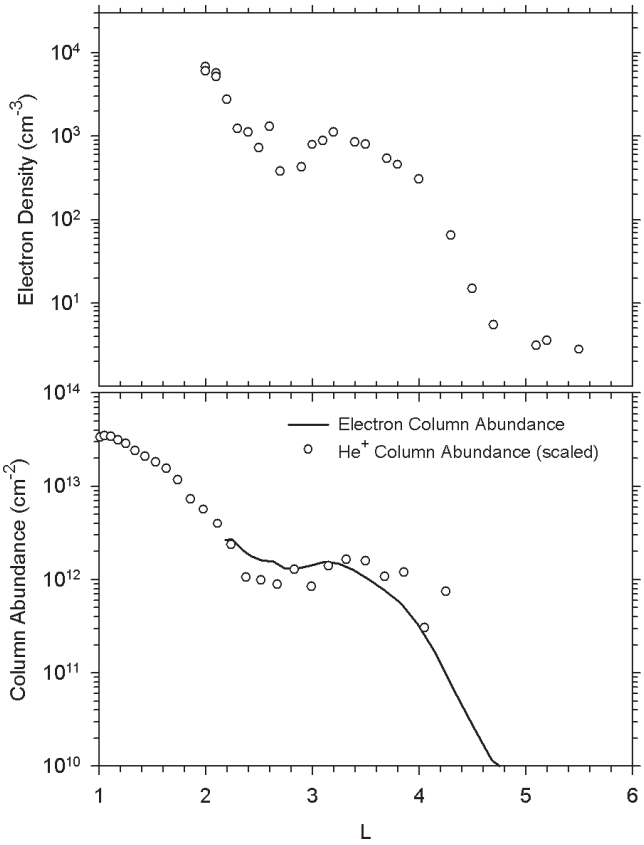

Figure 13. Similar to Figure 5 for 13 March 2001. The measured He^+ column abundance has been shifted to lower L by 1 unit before plotting.

during the period of high Kp may begin to corotate as Kp decreases. The preponderance of declining phases in Kp is likely a selection effect because identifying correlations between the EUV and RPI data in this analysis is more likely when plasma plumes are in near corotation.

[23] Our analysis illustrates several advantages of combining the RPI and EUV data. RPI provides a means of directly determining variations in electron number density across a convection plume. The EUV images represent line-of-sight integrations through the plasma. From a single image it is impossible to characterize the density structure along the line of sight. RPI data can give accurate electron densities along its trajectory through the plasmasphere from the spectrogram data alone. RPI data supplement EUV observations of plasma plumes by detecting density enhancements below the sensitivity threshold of the EUV cameras. This threshold was estimated by *Goldstein et al.* [2003] to be 40 ± 10 electrons cm^{-3} based on a comparison of RPI and EUV observations of shallow density gradients in the plasmasphere.

[24] The 27 June 2001 event clearly illustrates how RPI supplements EUV global observations. The horizontal line in Figure 2 is the estimated EUV sensitivity threshold of 40 electrons cm^{-3}. For this event, RPI was capable of providing density estimates in the trough down to a level roughly 10 times less than the EUV sensitivity limit. A trough model [*Sheeley et al.*, 2001] based on CRRES observations overlays the RPI density estimates. This model serves to confirm the estimates of trough densities made by RPI above and below the estimated EUV sensitivity threshold.

[25] Only a few of the many RPI-observed cases of density enhancements outside the plasmasphere could be associated confidently with EUV-observed plasma plumes. The first attempt at establishing a correlation between the two data sets is to see if the longitude of the EUV and RPI observed features are similar. The same analysis technique and assumptions were applied uniformly to the data used in panel b of Figures 4, 7, 10, and 12. These figures show the highly inclined orbital path of IMAGE projected onto the magnetic equatorial plane. These figures are created assuming that the plasma structures, shown as filled circles, maintained corotation between the time of the IMAGE spacecraft passage through the structure and the EUV observation period, often several hours later. Further analysis of sequential EUV images may provide estimates of the amount of error introduced by assuming these plasma plumes corotate. RPI data from the same plume will aid in this analysis by extending the baseline of observations by several hours. The orbital overlays are therefore not meant to show precisely where IMAGE crossed the convection plume but rather to show that there is a strong likelihood that the EUV and RPI-observed structures are indeed the same. Our model of the He^+ column abundance, using the RPI electron densities, was consistent with the structures measured by EUV. The adjustments that were made, as described in the text, were not only reasonable but should be expected.

[26] It must be understood that the densities derived from RPI spectrograms were not made at the equator but rather at midlatitudes. For the 27 June 2001 event, IMAGE entered this structure at a magnetic latitude of 25 degrees and exited the structure at a latitude of 33 degrees. It is clear from Figure 4b that the sharp rise in number density and the convection plume are correlated. Further work on establishing the amount of slippage from corotation the plumes experience as functions of radial distance will help to better align the two data sets.

[27] It should also be noted that not every enhancement of density seen in the trough by RPI is necessarily a plasma plume. EUV has observed a variety of structures such as "fingers" or "notches" in the plasmasphere [*Sandel et al.*, 2001]. A systematic survey of the RPI and EUV databases using the techniques discussed in this paper will aid in the identification of these other structures in RPI dynamic spectrograms.

[28] RPI has shown that the EUV-observed plasma plumes can have large latitudinal extent. Previous work never claimed that plasma plumes necessarily were confined to the equator, but what this new analysis provides is unambiguous confirmation that many density enhancements observed outside the plasmasphere at higher latitudes are plasma plumes. Given the long path length of He^+ through the plasmasphere, the latitudinal extent of these plasma plumes would be more difficult to appreciate using EUV data alone. Recent analysis of ionospheric maps of total electron content support the conclusion that the high density regions seen by EUV as plasma plumes do have large latitudinal extent along L shells even down to the ionosphere [*Foster et al.*, 2002].

5. Conclusions

[29] The paradigm for studies of the plasmasphere over the past 30 years has been to make local observations of the

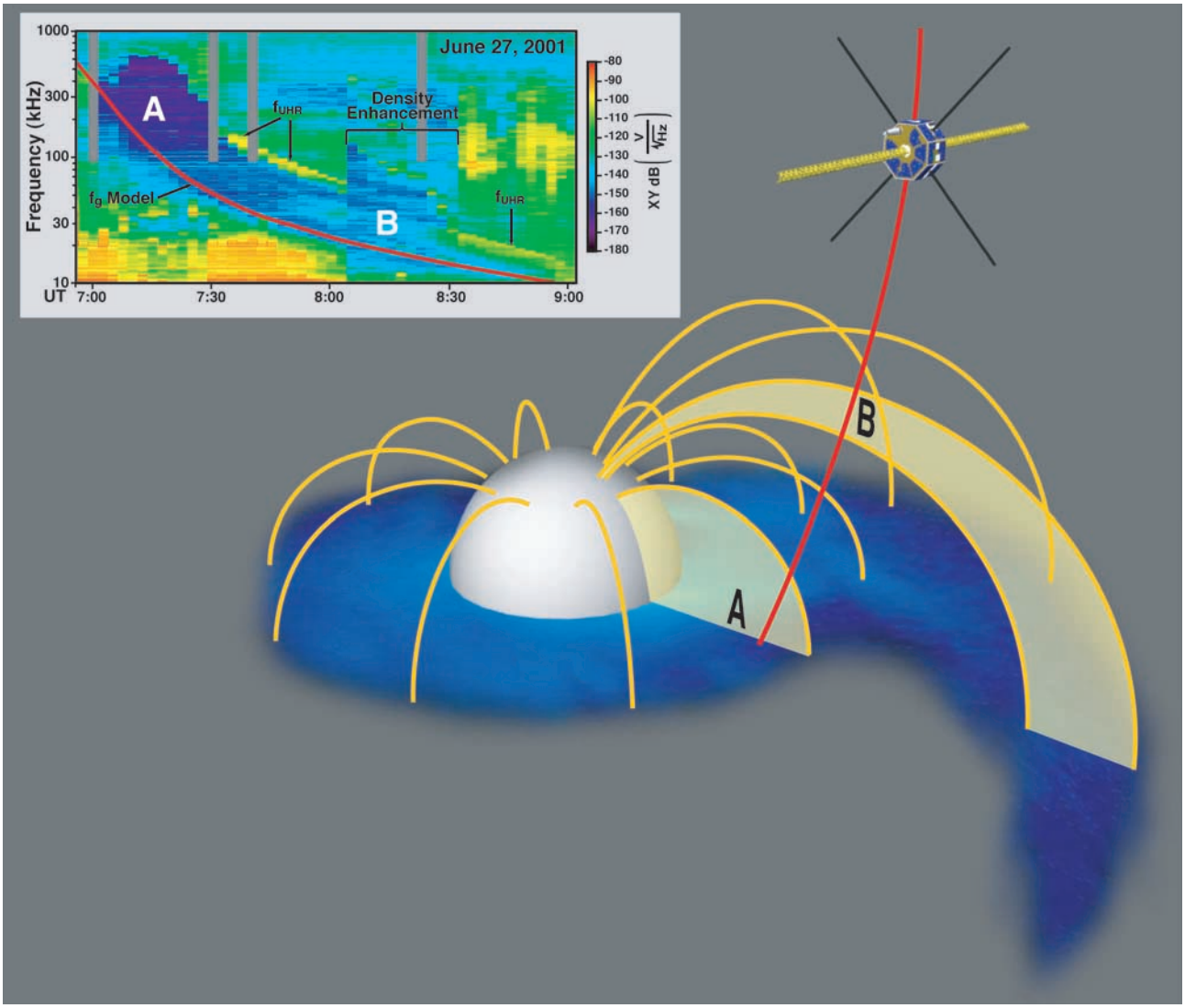

Figure 14. A schematic of the IMAGE orbit (in red) crossing the magnetic field lines threading through the plasmasphere (region A) and the plasma convection plume (region B). The density enhancements seen by RPI are on the same field lines as the plasma plume observed by EUV but at high latitudes. The field-aligned density enhancements are shown shaded in yellow. An EUV observed plasmasphere image for 27 June 2001 is here projected onto the magnetic equatorial plane. An RPI spectrogram for the same day similar to that shown in Figure 1 is reproduced here with the labels A and B corresponding to the plasmasphere and plasma plume, respectively.

plasmasphere and use models to estimate its global characteristics. Multiple samples of local plasmaspheric conditions can give more confidence in the model but deconvolving the temporal and spatial variations in the data may be difficult. The perspective gained by using global images provided by the EUV cameras on the IMAGE spacecraft allow the temporal and spatial variations of the plasmasphere to be clearly observed. RPI data allow for local measurements of the plasmasphere to be made within a few hours of these global images and aid in the interpretation of EUV data. Figure 14 is a schematic of the IMAGE orbit crossing magnetic field lines threading through the plasma convection plume. It is during these times that RPI detects large density enhancements. By combining these two data sets in the study of density enhancements outside the plasmasphere, we demonstrate that these apparently detached plasma density structures, seen in many RPI dynamic spectrograms, often represents the high-latitude extension of plasma convection plumes. We demonstrate the complementary local/global relationship of RPI and EUV observations in determining the structure of plasma convection plumes.

[30] **Acknowledgments.** The authors would like to acknowledge Dennis Gallagher for software which aided in analysis of the EUV data; Vivek Dwivedi for help in preparation of figures used in this paper; and Timothy Eastman, Jerry Goldstein, and our two reviewers for constructive comments on the manuscript. L. N. G. was supported by NASA contract NAS5-98156 by subcontract from Raytheon ITSS. B. W. R. and B. R. S. were supported under NASA contract NAS5-9602 by subcontract with Southwest Research Institute. This research has made use of data obtained from the CDAWeb provided by NASA's Goddard Space Flight Center.

[31] Arthur Richmond thanks the reviewers for their assistance in evaluating this paper.

References

Carpenter, D. L., and R. R. Anderson, An ISEE/whistler model of equatorial electron density in the magnetosphere, *J. Geophys. Res.*, *97*, 1097–1108, 1992.

Carpenter, D. L., B. L. Giles, C. R. Chappell, P. M. E. Décréau, R. R. Anderson, A. M. Persoon, A. J. Smith, Y. Corcuff, and P. Canu, Plasmasphere dynamics in the duskside bulge region: A new look at an old topic, *J. Geophys. Res.*, *98*, 19,243–19,271, 1993.

Carpenter, D. L., R. R. Anderson, W. Calvert, and M. B. Moldwin, CRRES observations of density cavities inside the plasmasphere, *J. Geophys. Res.*, *105*, 23,323–23,338, 2000.

Chappell, C. R., Detached plasma regions in the magnetosphere, *J. Geophys. Res.*, *79*, 1861–1869, 1974.

Chen, A. J., and J. M. Grebowsky, Plasma tail interpretations of pronounced detached plasma regions measured by OGO 5, *J. Geophys. Res.*, *79*, 3851–3855, 1974.

Chen, A. J., and R. A. Wolf, Effects on the plasmasphere of a time-varying convection electric field, *Planet. Space Sci.*, *20*, 483–509, 1972.

Foster, J. C., P. J. Erickson, A. J. Coster, J. Goldstein, and F. J. Rich, Ionospheric signatures of plasmaspheric tails, *Geophys. Res. Lett.*, *29*(13), 1623, doi:10.1029/2002GL015067, 2002.

Fung, S. F., L. N. Garcia, J. L. Green, D. L. Gallagher, D. L. Carpenter, B. W. Reinisch, I. A. Galkin, G. Khmyrov and B. R. Sandel, Plasmaspheric electron density distributions sampled by Radio Plasma Imager on the IMAGE satellite, *EOS Trans. AGU*, *82*(47), Fall Meet. Suppl., abstract SMIIA-0771, 2001.

Fung, S. F., et al., Observations of magnetospheric plasmas by the radio plasma imager (RPI) on the IMAGE mission, *Adv. Space Res.*, *30*, 2259–2266, 2002.

Galkin, I., G. Khmyrov, A. Kozlov, B. Reinisch, X. Huang, and G. Sales, New tools for analysis of space-borne sounding data, paper presented at 2001 National Radio Science Meeting, USNC/URSI, Boston, Mass., 8–13 July 2001.

Goldstein, J., M. Spasojevic, P. H. Reiff, B. R. Sandel, W. T. Forrester, D. L. Gallagher, and B. W. Reinisch, Identifying the plasmapause in IMAGE EUV data using IMAGE RPI in situ steep density gradients, *J. Geophys. Res.*, *108*(A4), 1147, doi:10.1029/2002JA009475, 2003.

Grebowsky, J. M., Model study of plasmapause motion, *J. Geophys. Res.*, *75*, 4329–4333, 1970.

Grebowsky, J. M., and A. J. Chen, Effects on the plasmasphere of irregular electric fields, *Planet. Space Sci.*, *24*, 689, 1976.

Gurnett, D. A., R. R. Anderson, F. L. Scarf, R. W. Fredricks, and E. J. Smith, Initial results from the ISEE-1 and -2 plasma wave investigation, *Space Sci. Rev.*, *23*, 103–122, 1979.

Ho, D., and D. L. Carpenter, Outlying plasmasphere structure detected by whistlers, *Planet. Space Sci.*, *24*, 987–994, 1976.

Horwitz, J. L., R. H. Comfort, and C. R. Chappell, A statistical characterization of plasmasphere density structure and boundary locations, *J. Geophys. Res.*, *95*, 7937–7947, 1990.

Maynard, N. C., and A. J. Chen, Isolated cold plasma regions: Observations and their relation to possible production mechanisms, *J. Geophys. Res.*, *80*, 1009–1013, 1975.

Mosier, S. R., M. L. Kaiser, and L. W. Brown, Observations of noise bands associated with the upper hybrid resonance by the Imp 6 radio astronomy experiment, *J. Geophys. Res.*, *78*, 1673–1679, 1973.

Reinisch, B. W., et al., The Radio Plasma Imager investigation on the IMAGE spacecraft, *Space Sci. Rev.*, *91*, 319–359, 2000.

Reinisch, B. W., et al., First results from the Radio Plasma Imager on IMAGE, *Geophys. Res. Lett.*, *28*, 1167–1170, 2001.

Sandel, B. R., et al., The Extreme Ultraviolet Imager investigation for the IMAGE mission, *Space Sci. Rev.*, *91*, 197–242, 2000.

Sandel, B. R., R. A. King, W. T. Forrester, D. L. Gallagher, A. L. Broadfoot, and C. C. Curtis, Initial results from the IMAGE Extreme Ultraviolet Imager, *Geophys. Res. Lett.*, *28*, 1439–1442, 2001.

Sandel, B. R., J. Goldstein, D. L. Gallagher, and M. Spasojevic, Extreme ultraviolet imager observations of the structure and dynamics of the plasmasphere, *Space Sci. Rev*, in press, 2003.

Sheeley, B. W., M. B. Moldwin, and H. K. Rassoul, An empirical plasmasphere and trough density model: CRRES observations, *J. Geophys. Res.*, *106*, 25,631–25,641, 2001.

Spasojevic, M., J. Goldstein, D. L. Carpenter, U. S. Inan, B. R. Sandel, B. W. Reinisch, and R. R. Anderson, Duskside outer plasmaspheric structure observed in global images and in situ, *EOS Trans. AGU*, *83*(19), Fall Meet. Suppl., abstract SM418-10, 2002.

Taylor, H. A., J. M. Grebowsky, and W. J. Walsh, Structured variations of the plasmapause: Evidence of a corotating plasma tail, *J. Geophys. Res.*, *76*, 6806–6814, 1971.

Tsyganenko, N. A., Modeling the Earth's magnetospheric magnetic field confined within a realistic magnetopause, *J. Geophys. Res.*, *100*, 5599–5612, 1995.

S. A. Boardsen, L-3 Communications EER Systems, Inc./NASA Goddard Space Flight Center, Code 630, Greenbelt, MD 20771, USA. (Scott.A.Boardsen@gsfc.nasa.gov)

S. F. Fung and J. L. Green, NASA Goddard Space Flight Center, Code 630, Greenbelt, MD 20771, USA. (Shing.F.Fung@nasa.gov; James.L.Green@nasa.gov)

L. N. Garcia, QSS Group, Inc./NASA Goddard Space Flight Center, Code 630, Greenbelt, MD 20771, USA. (Leonard.Garcia@gsfc.nasa.gov)

B. W. Reinisch, Center for Atmospheric Research, University of Massachusetts, Lowell, MA 01854, USA. (Bodo_Reinisch@uml.edu)

B. R. Sandel, Lunar and Planetary Laboratory, The University of Arizona, Tucson, AZ 85721, USA. (sandel@vega.lpl.arizona.edu)